CONF-810602--21

LA-UR -81-839

TITLE: BURNING AND DETONATION

MASTER

AUTHOR(S): Charles A. Forest

SUBMITTED TO: Symposium on Detonation, Annapolis, MD, June 16-19, 1981

University of California

LOS ALAMOS SCIENTIFIC LABORATORY
Post Office Box 1663 Los Alamos, New Mexico 87545
An Affirmative Action/Equal Opportunity Employer

Form No. 836 R3
St. No. 2629
12/78

UNITED STATES
DEPARTMENT OF ENERGY
CONTRACT W-7405-ENG-36

BURNING AND DETONATION

Charles A. Forest
Los Alamos National Laboratory
Los Alamos, New Mexico

The effect of confined burning explosive abutting non-burning explosive in a variety of one-dimensional geometries has been studied by numerical simulation, demonstrating the effects of confinement, burning rate, and shock sensitivity. The model includes porous bed burning, compressible solids and gases, shock-induced decomposition with possible transition to detonation, and constant velocity ignition fronts. Two-phase flow, gas relative to solid, is not allowed.

Because the shock sensitivity of an explosive changes with explosive density and because such experimental data is rarely available over a range of densities, a method for the calculation of the density effect on the initial-shock-pressure, distance-to-detonation (wedge test) measure of shock sensitivity is given. The calculation uses the invariance with density of the shock particle velocity as a function of time to detonation, and the experimental data at some high density.

INTRODUCTION

Some models of the deflagration-to-detonation transition (DDT) for porous, solid explosives have involved complicated convective combustion models but lacked the inclusion of any model of what is usually called only shock initiation of detonation. In these models, the occurrence of some rapid pressure increase to a high pressure by way of convective combustion was taken as sufficient to mark the onset of detonation (1,2). Others have envisioned DDT to be marked by initial convective combustion, then low-velocity detonation (LVD), and finally detonation (3,4). This study takes another approach that employs a simple burning model but includes a shock induced decomposition rate model derived from shock initiation experiments, which allows detonation to occur as a reactive shock growth process. This is somewhat similar to the LVD picture (although here a rate model is employed to calculate the accelerating shock), but is in contrast to the convective wave pressure, runaway model. The shock growth may occur in the porous bed itself or in some region of explosive abut to the burning region in which no convective burn may have occurred at all. Because the burning is modeled separately from the initiation mechanism, this approach is called simply "burning and detonation."

Specifically, the model has four distinct features: (1) separate compressible equations of state are used for the solid undecomposed explosive and for the gaseous products with pressure-temperature equilibrium assumed for mixtures of the two; (2) the burn of explosive takes place on the surface of particles according to a (P^n) rate and is uniformly ignited throughout or is ignited following an ignition front; (3) no gas flow is allowed relative to the solid, product gases remain where they are formed; and (4) shock induced decomposition of the solid is allowed as a mass decomposition rate process accelerating the shocks initially formed by the burning porous bed. The models used for each of these features and the limits of applicability for each are discussed separately in the following sections.

EQUATION OF STATE

The HOM (5) equation of state is used throughout the calculations with pressure given as a function of specific volume (V), specific internal energy (I), and mass fraction of solid (W), P = H(V,I,W). Only two phases are allowed, solid and gas with reacting explosives being represented as some mixture of undecomposed solid and product gas. Solids are represented by a Grüneisen expansion off the shock Hugoniot with temperature calculated by the Walsh and Christian (6) technique; thus

$$P_s(V_s, I_s) = \Gamma(I_s - I_H(V_s))/V_s + P_H(V_s) \quad (1)$$

and

$$T_s(V_s, I_s) = (I_s - I_H(V_s))/C_{V_s} + T_H(V_s) \quad , (2)$$

where V_s = specific volume of solid, I_s = specific internal energy of solid, I_H = specific Hugoniot energy, T_H = Hugoniot temperature. For the case of solid only, $V_s = V$, $I_s = I$, and $W = 1$. Gas products are represented by a Beta equation of state off the BKW (7,8) calculated detonation isentrope. Thus,

$$P_g(V_g, I_g) = (I_g - I_i(V_g))/(\beta(V_g) \cdot V_g) + P_i(V_g) \quad (3)$$

and

$$T_g(V_g, I_g) = (I_g - I_i(V_g))/C_{V_g} + T_i(V_g) \quad , \quad (4)$$

where V_g = specific volume of gas, I_g = specific internal energy of gas, I_i = specific energy on the isentrope, P_i = pressure on the isentrope, and T_i = temperature on the isentrope. For the case of gas only, $V = V_g$, $I = I_g$, and $W = 0$. Mixtures of gas and solid are calculated by simultaneous solution of the gas and solid equations for pressure and temperature equilibrium, assuming ideal partition of volumes and energies. Thus, for mixtures,

$$P_s(V_s, I_s) = P_g(V_g, I_g) \quad (5)$$

and

$$T_s(V_s, I_s) = T_g(V_g, I_g) \quad , \quad (6)$$

where

$$V = WV_s + (1 - W)V_g \quad (7)$$

and

$$I = WI_s + (1 - W)I_g \quad . \quad (8)$$

Porous material is subject to compaction and porous bed compaction has been observed in DDT experiments. The representation of the solid in the HOM equation of state does allow compaction and so simulates this important feature of the porous bed behavior.

POROUS BED BURN

The porous explosive is burned according to the surface regression rate $\dot{X} = CP^n$ with some initial surface-to-volume $(S/V)_0$ ratio. Thus, $dW/dt = -(S/V)_0 (W)^q CP^n$, where q is an exponent dependent upon the particle geometry. For sphere-like particles (any particle having an inscribed cylinder), q = 1/2. For planar particles (sheets), q = 0. The W^q term accounts for the change in surface-to-volume ratio as the particle burns, although in the calculations this term is relatively unimportant because detonation occurs when W is still close to 1.0. As a brief development of this form, expand the mass burn rate dM/dt as follows:

$$dM/dt = -S\rho\dot{X} \quad (9)$$

and then

$$dM/dt = -(S_0/V_0)(S/S_0)(\rho_0 V_0)(\rho/\rho_0)\dot{X} \quad , \quad (10)$$

where S = surface area, V = volume, and ρ = density. The subscript 0 indicates the initial values. Note that $W = M/M_0 = M/(\rho_0 V_0)$ and that (ρ/ρ_0) is very close to 1.0 for the pressure range of burning. Thus

$$dW/dt = -(S/V)_0 (S/S_0)\dot{X} \quad . \quad (11)$$

An approximation for the surface area term is $(S/S_0) = W^q$, for some q. The motivation for this is shown by considering sphere-like particles; thus, for some A,

$$S = Ar^2 \quad ,$$

$$V = Ar^3/3 \quad , \text{ and} \quad (12)$$

$$(S/S_0) = (r/r_0)^2 = (\rho V/\rho_0 V_0)^{2/3} = W^{2/3} \quad ,$$

where r = radius of the inscribed sphere. Particular examples of sphere like particles are cubes (A = 24), tetrahedra (A = $24\sqrt{3}$), and spheres (A = 4π). The treatment of cylinder-like particles is similar.

Ignition is simply the onset of burning in this model with no account of ignition processes. For some problems ignition is taken to be complete throughout the porous bed region, while in others burning commences following the spread of a constant velocity "ignition

front wave." In short, in this model ignition is the onset of rapid burning.

GAS FLOW

No gas flow through the porous bed is allowed; the product gases remain with the solids from which they were generated. This assumption is reasonable for cases in which the ignition is uniform over the porous bed. For the cases where the ignition front spreads at constant velocity, the assumption is somewhat inconsistent because some gas flow is needed for ignition processes. However, if the fraction of mass involved in ignition is small, then in regard to fluid dynamics the gas flow can be ignored. The inclusion of gas flow relative to the solid would, of course, affect principally the initial stages of burning where there is a small amount of gas escaping into the pores; at later times the flow would be relatively reduced as the gas fills the pores and as the gas evolution rate exceeds the transport rate through the pores. Compaction of the porous bed, of course, also limits gas flow.

SHOCK-INDUCED DECOMPOSITION

Shock-induced decomposition is calculated by the Forest Fire (9,10) reaction rate model (a name coined by a few enthusiastic users), a one-step, solid-to-products decomposition rate calculated using the HOM equation of state, the experimentally determined $U_S = C + SU_p$ Hugoniot, and the wedge test (11,12) determined graph of distance to detonation (mm) versus initial shock pressure (P). The graph of ln (mm) versus ln (P) is often a straight line, ln (mm) = a + b ln (P), and is called the Pop plot for Alphonse Pepolato (13). Briefly, the Forest Fire rate is the explosive decomposition rate necessary behind a planar shock wave to accelerate the shock wave along the time-distance-state space curve determined by the Pop plot and Hugoniot, interpreting the Pop plot as a shock pressure growth curve. The rate also depends upon the pressure gradient following the shock front; for instance, where the pressure gradient is unknown, an accelerating square wave is assumed. The rate is fit as a function of shock pressure but is extended to the region behind the shock as a function of local pressure.

An abbreviated analysis for Forest Fire follows; more detailed accounts are given in Refs. 9 and 10. The analysis centers upon accelerating sharp planar shocks with the following fluid dynamics represented in Lagrange mass-time (m,τ) coordinates defined by

$$m = \int_{x_0(t)}^{x} \rho(x',t)\,dx'$$

and (13)

$$\tau = t \ ,$$

where $x_0(t)$ is the trajectory of some mass point. In these coordinates the fluid flow equations are

$$U_\tau = -P_m \ ,$$

$$V_\tau = U_m \qquad (14)$$

and

$$I_\tau = -PV_\tau \ .$$

Here the subscripts denote partial differentiation, the τ derivative is the time derivative at constant mass. Thus, the reaction rate is W_τ and occurs in the time differentiation of the equation of state

$$P = H(V,I,W) \ , \qquad (15)$$

and

$$P_\tau = H_V V_\tau + H_I I_\tau + H_W W_\tau \ . \qquad (16)$$

It is sufficient to determine P_τ, V_τ, and I_τ for solution of W_τ; the solution proceeds then by determining those derivatives from differentiation of the pressure (P) and the particle velocity (U) on the shock line. Let $m_S(\tau)$ be the mass position of the shock so that $\dot{m}_S = \rho_0 U_S$. Then,

$$\dot{P} = dP(m_S(\tau),\tau)/d\tau = \rho_0 U_S P_m + P_\tau \qquad (17)$$

and

$$\dot{U} = dU(m_S(\tau),\tau)/d\tau = \rho_0 U_S U_m + U_\tau \ . \qquad (18)$$

The derivatives $\dot{P}$ and $\dot{U}$ are obtained from the Pop-plot, Hugoniot, and shock jump equation,

$$\dot{P} = -\frac{dP}{d\,mm}\frac{d\,mm}{d\tau} = -\frac{dP}{d\,mm}U_S$$

and (19)

$$\dot{P} = \rho_0(c + 2sU)\dot{U} \ .$$

Finally, then,

$$P_\tau = \dot{P} - \rho_0 U_S P_m \ , \qquad (20)$$

$$V_\tau = U_m = (\dot{U} + P_m)/(\rho_0 U_S) \ , \qquad (21)$$

and

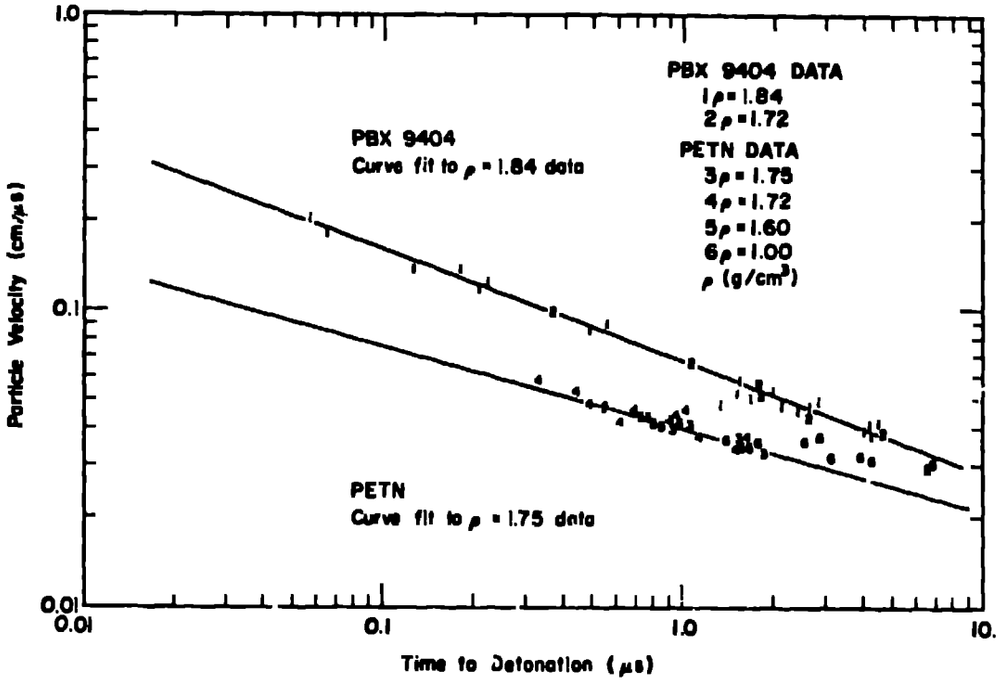

Fig. 2 - Shock particle velocity vs time to detonation showing the invariance of the graph with different densities.

The graph run versus P is the estimated Pop plot, Fig. 1. The graph of run versus tdet is the shock locus, Figs. 3 and 4. In the figures, the solid lines are calculated using the $U_p = F(t)$ function and Hugoniot from the highest (higher) density data. The points are wedge test data (12,15). Note that the Pop plot is constructed, even at the reference density, from the particle velocity function and is not the $\ln(\text{run}) = a + b \ln(P)$ relation usually used in least-square fits of the Pop plot.

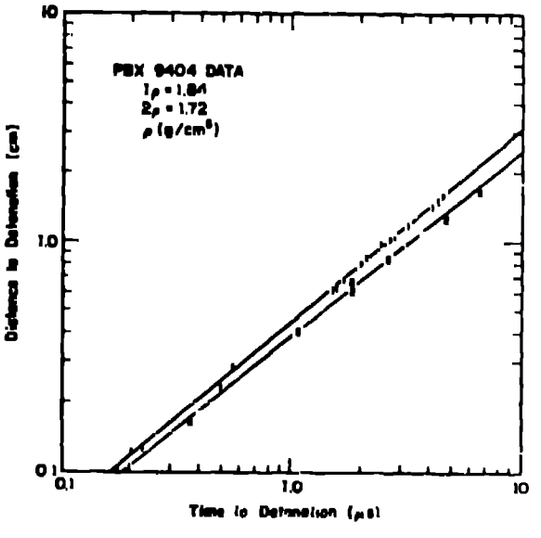

Fig. 3 - Calculated distance to detonation for PBX 9404 based on the data at $\rho = 1.84$.

CALCULATIONS

Five model calculations made with the SIN (5) one-dimensional fluid dynamics code on VOP 7 systems examine the effect of surface-to-volume ratio in the porous bed burn, the change of shock sensitivity in the nonburning adjacent explosive, and the effect of cylindrical convergence and divergence. In Fig. 5 is shown the experiment Pop plot and a calculated Pop plot for VOP 7 at a lower density, using the Pop plot estimation

$$I_\tau = -PV_\tau \quad . \qquad (22)$$

If P_m is unknown, the case of $P_m \equiv 0$ is taken. The solution for W_τ is complete. In practice, $-W_\tau/W$ is fit as a function of shock pressure.

The shock sensitivity of a solid explosive is greatly influenced by its initial density; with lower density the sensitivity is greater and this change is apparent from the pop plots, Fig. 1. This property is often used in the design of explosive devices to adjust the sensitivity of explosive components and it also, in part, gives reason to the concern to make uniform density charges. In the case of porous beds in DDT situations, the initial burn products can compact the porous bed with nonshock pressure waves. The compacted region may well vary in density throughout the region, which gives, correspondingly, a varying shock sensitivity. The varying sensitivity implies that the shock-induced decomposition rate function is also dependent upon the local preshock density at the time that the first shock passes the point. This observation is problematic, especially in numerical methods where shocks are spread out, because some distinction need then be made between ramp, slow compressive waves and shock waves.

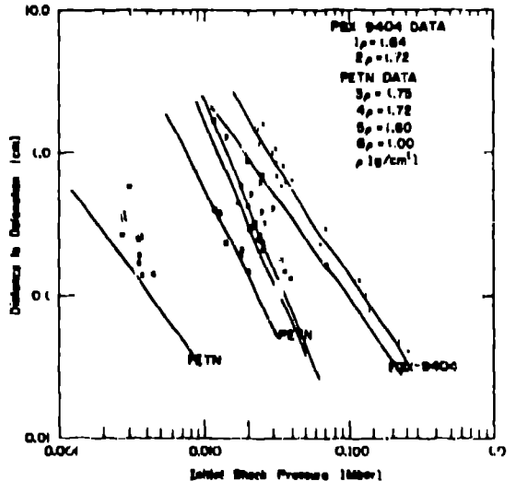

Fig. 1 - Calculated Pop plots for PBX 9404 and PETN. The lines are calculated from data at the highest density for each explosive.

A brief description of a method to calculate the Pop-plot change with density is given here; a more detailed account is found in Ref. 10. The method centers on the assumption that shock particle velocity as a function of time to detonation, $U_p = F(t)$, is independent of initial density for the wedge test data. The assumption is based on observation of data displayed in Fig. 2, whereupon is plotted data for PBX 9404 at two densities and for PETN at four densities. Also key to the method is the estimation of the shock Hugoniot line at a lower density ρ_2 from data at some higher reference density ρ_1 (14).

Let the pressure P be the independent variable at the shock front. Solve for V from

$$P = P_H(V) \cdot G(V) \quad , \qquad (23)$$

where

$P_H(V)$ = Hugoniot pressure at reference density ρ_1,

$$G(V) = \frac{2V - \Gamma(V_1 - V)}{2V - \Gamma(V_2 - V)} \quad ,$$

$V_1 = 1/\rho_1$,

$V_2 = 1/\rho_2$,

and

Γ = Grüneisen constant. Then

$$U_p = |P(V_2 - V)|^{\frac{1}{2}} \qquad (24)$$

and

$$U_s = V_2 |P/(V_2 - V)|^{\frac{1}{2}} \qquad (25)$$

Solve time to detonation, t_{det}, from

$$U_p = F(t_{det}) \quad . \qquad (25)$$

Finally, after a sufficient table of (t_{det}, U_s) is formed, integrate numerically

$$run = \int_0^{t_{det}} U_s dt \quad .$$

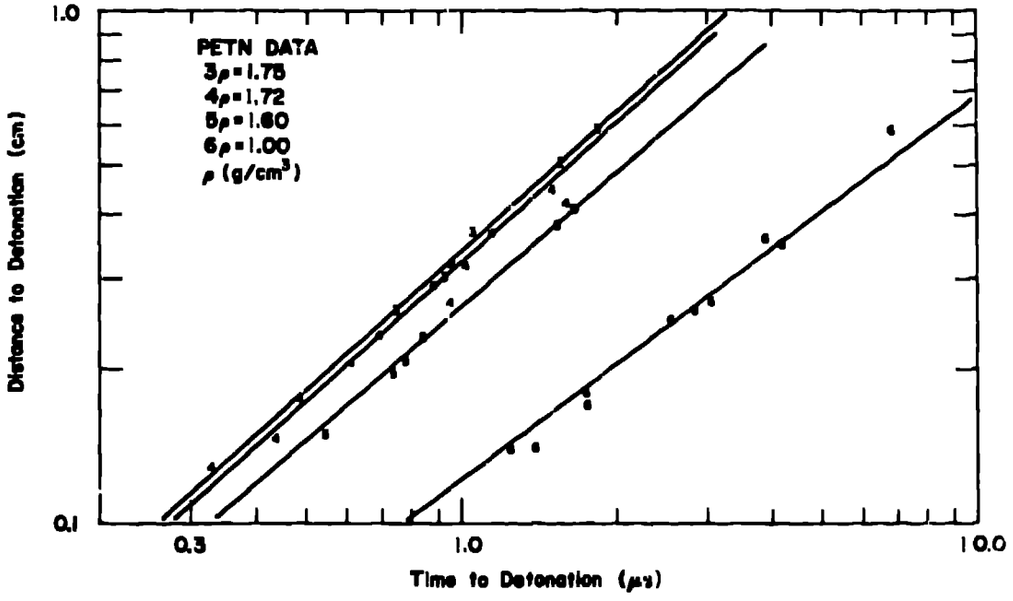

Fig. 4 - Calculated distance to detonation vs time to detonation for PETN based on the data at $\rho = 1.75$.

method mentioned earlier. In Fig. 6 are shown the porous bed burn decomposition rates and the Forest Fire shock-induced decomposition rates. The problem geometries and material regions are shown in Fig. 7. Problem geometries I and II are planar; problem geometries III and IV are cylindrical, with the cylindrical axis at the left. Input constants are listed in Ref. 10.

The first two calculations, Figs. 8 and 9, show the change in behavior with a small change in $(S/V)_0$ in the porous bed burn and utilize problem geometry I (Fig. 7). In Fig. 8, the pressure wave from the uniformly burning bed is sufficient to induce a shock transition to detonation in the solid VOP 7. In Fig. 9 the pressure wave is not sufficient to induce a detonation.

The third calculation uses problem geometry II (Fig. 10), which is similar to problem geometry I but includes a 1-cm region of lower density VOP 7. The lower density region, $\rho_0 = 1.72$ g/cm^3, is more shock sensitive and has a higher shock-induced decomposition rate, Fig. 6. The porous bed has $(S/V)_0 = 75$ cm^{-1}, the same $(S/V)_0$ that resulted in a failure to detonate in the previous problem. In this case, however, the increased reaction in the $\rho_0 = 1.72$ Forest Fire region

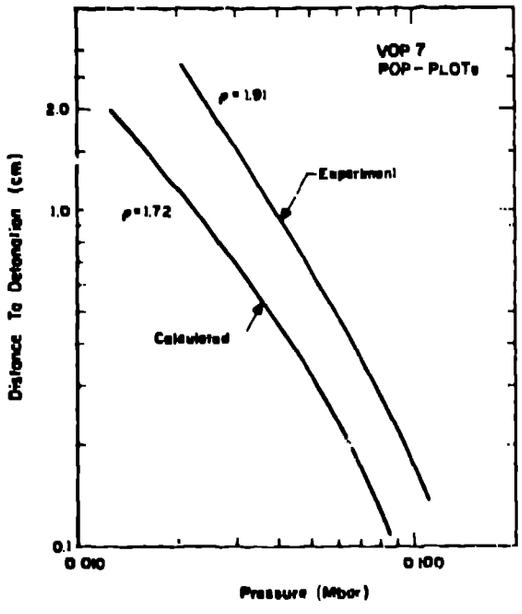

Fig. 5 - Distance to detonation as a function of initial shock pressure. The experimental line is from Los Alamos wedge test data (15). The $\rho_0 = 1.72$ line is calculated using the $\rho_0 = 1.91$ data.

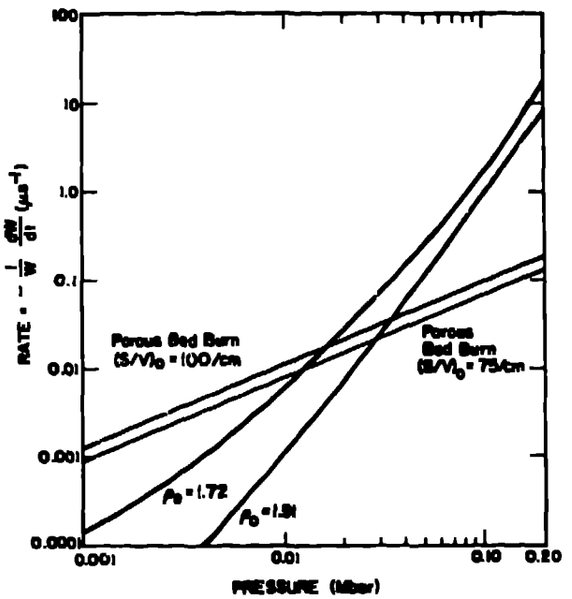

Fig. 6 - Forest Fire and porous bed burn decomposition rates. The two curves ρ_0 = 1.91 and ρ_0 = 1.72 are Forest Fire rates based on the Pop plot of Fig. 5. The porous bed burn rates are the initial W = 1 rates.

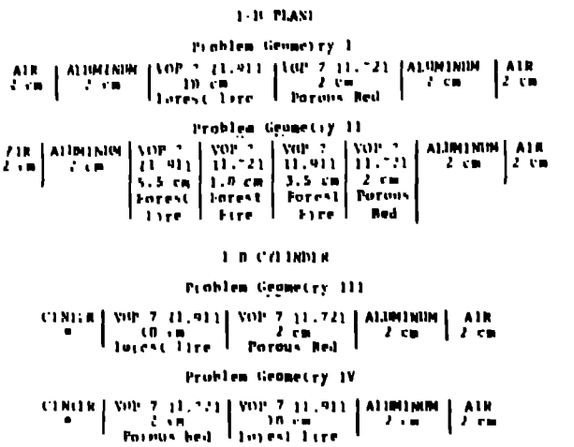

Fig. 7 - Problem geometries for VOP 7 burning and detonation.

boosts the shock wave growth enough to cause detonation to occur farther along into the next high-density VOP 7 region. Note that detonation did not occur in the low density region, but the presence of that region was sufficient to alter the outcome.

The fourth calculation is again similar to the first problem but the

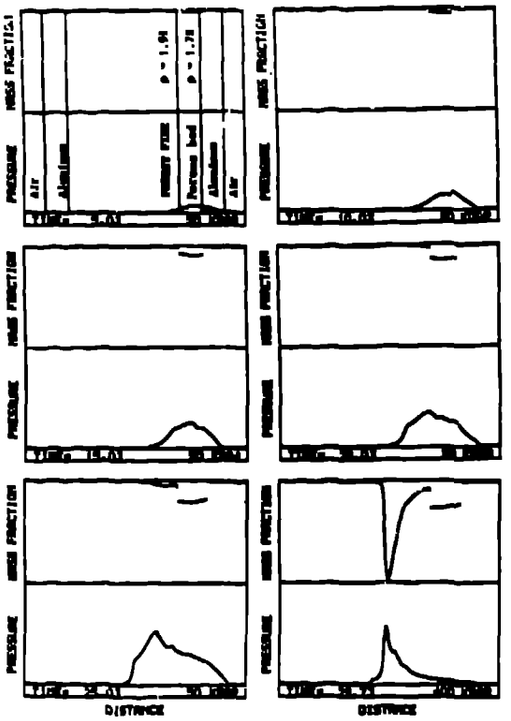

Fig. 8 - SIN calculation for a 1-D plane in problem geometry I with $(S/V)_0$ = 100 cm.

geometry has been changed to one-dimensional, cylindrical, problem geometry III. In Fig. 11 the porous bed has $(S/V)_0$ = 75, again the case that failed in planar geometry. However, in this instance, the inward running shock pressure is increased by cylindrical convergence and a transition to detonation occurs.

The fifth calculation is also in cylindrical geometry, problem geometry IV. In Fig. 12, the burning region is at the center of the cylinder and has $(S/V)_0$ = 100 cm^{-1}. This $(S/V)_0$ was sufficient to induce detonation in the planar case; but due to the cylindrical divergence of the wave, no detonation occurs.

In other calculational studies, this burning to-detonation model and the two-dimensional Lagrangian hydrodynamic code 2DL (16) have been used to investigate the detonation of a solid propellant grain from shocks induced by a burning porous bed (17) and to calculate the burning and detonation in an all-PETN hot-wire assembly (18).

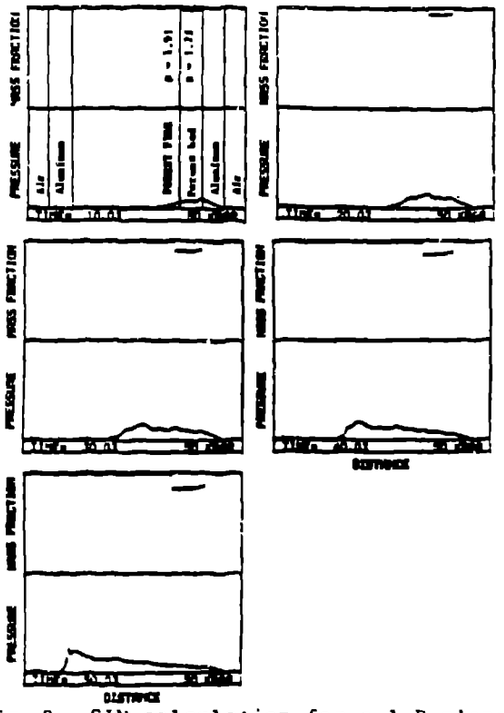

Fig. 9 - SIN calculation for a 1-D plane in problem geometry I with $(S/V)_0$ = 75/cm.

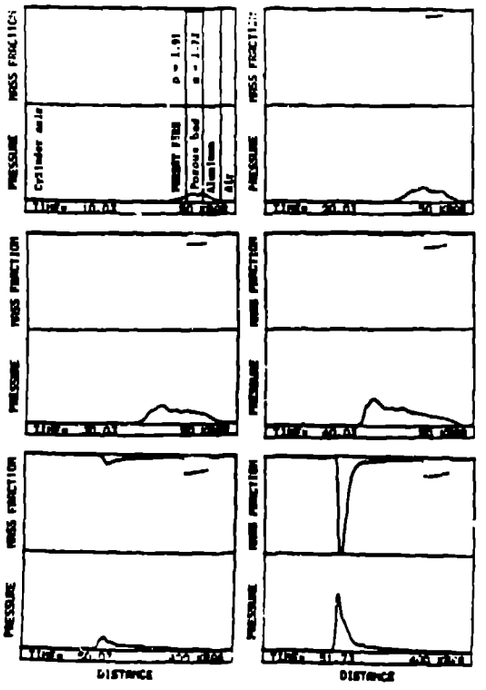

Fig. 11 - SIN calculation for a 1-D cylinder in problem geometry III with $(S/V)_0$ = 75/cm.

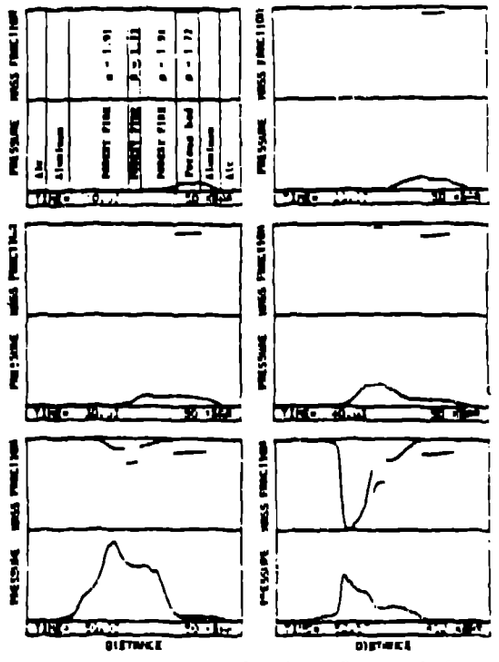

Fig. 10 - SIN calculation for a 1-D plane in problem geometry II with $(S/V)_0$ = 75/cm.

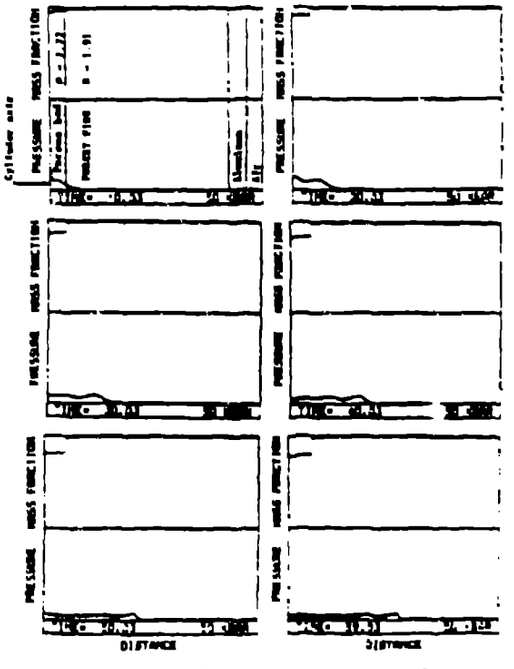

Fig. 12 - SIN calculation for a 1-D cylinder in problem geometry IV with $(S/V)_0$ = 100/cm.

CONCLUSIONS

The model calculations indicate that there is some burning rate in a porous bed of explosive that is sufficient to cause shock-induced detonation in an adjacent region of explosive which itself is not burning. The burning rate necessary to induce the detonation is dependent upon shock sensitivity, geometry, and confinement. These features are expected to be important to modeling DDT in porous beds where initial product gases compact part of the porous bed, giving a region of varying shock sensitivity. Also, the transition from shock to detonation may be at a distance from the burning region.

REFERENCES

1. D. T. Pilcher, M. W. Beckstead, L. W. Christensen, and A. J. King, "A Comparison of Model Predictions and Experimental Results of DDT Tests," Sixth Symposium (International) on Detonation, ACR-221, p. 258, 1976.

2. H. Krier and S. S. Gokhale, "Modeling of Convective Mode Combustion through Granulated Propellant to Predict Detonation Transition," AIAA Journal, Vol. 16, p. 177, 1978.

3. A. A. Sulimov, B. S. Ermolaev, A. A. Borisov, A. I. Korotkov, B. A. Khasainov, and V. E. Khrapovsky, "On the Mechanism of Deflagration to Detonation Transition in Gas-Permeable High Explosive," Sixth Symposium (International) on Detonation, ACR-221, p. 250, 1976.

4. A. F. Belyaev, V. K. Boholev, A. I. Korotkov, A. A. Sulimov, and S. V. Chuiko, "Transition from Deflagration to Detonation in Condensed Phases," translation TT74-50028, U.S. Dept. of Commerce, National Technical Information Service, Springfield, VA 22151.

5. Charles L. Mader and Milton Samuel Shaw, "User's Manual for SIN," Los Alamos National Laboratory Rept. LA-7264-m, Sept. 1978.

6. John M. Walsh and Russell H. Christian, "Equation of State of Metals from Shock Wave Measurements," Phys. Rev., Vol. 97, p. 1554, 1955.

7. Charles L. Mader, "FORTRAN BKW: A Code for Computing the Detonation Properties of Explosives," Los Alamos National Laboratory Rept. LA-3704, July 1967.

8. Charles L. Mader, "Detonation Properties of Condensed Explosives Computed Using the Becker-Kistiakowsky-Wilson Equation of State," Los Alamos National Laboratory Rept. LA-3704, July 1967.

9. Charles L. Mader and Charles A. Forest, "Two-Dimensional Homogeneous and Heterogeneous Detonation Wave Propagation," Los Alamos National Laboratory Rept. LA-6259, p. 60 (App. C), June 1976.

10. Charles A. Forest, "Burning and Detonation," Los Alamos National Laboratory Rept. LA-7245, p. 22 (App. B), July 1978.

11. A. W. Campbell, W. C. Davis, J. B. Ramsay, J. R. Travis, "Shock Initiation of Solid Explosives," Third Symposium on Detonation, ONR Rept. ACR-52, Vol. 2, p. 498.

12. G. E. Seay, L. B. Seely, "Initiation of Low-Density PETN Pressings by a Plane Shock Wave," Third Symposium on Detonation, ONR Rept. ACR-52, Vol. 2, p. 564.

13. J. B. Ramsay and A. Popolato, "Analysis of Shock Wave and Initiation Data for Solid Explosives," Fourth Symposium on Detonation, ACR-126, p. 233, 1965.

14. John O. Erkman and David J. Edwards, "Computed and Experimental Hugoniots for Unreacted Porous High Explosive," Sixth Symposium (International) on Detonation, ACR-221, p. 766, 1976.

15. Terry R. Gibbs and Alphonse Popolato, Editors, LASL Explosive Property Data, University of California Press, 1980.

16. Charles L. Mader, Numerical Modeling of Detonations, University of California Press, Berkeley, 1979.

17. Charles A. Forest, "A Model of Burning and Detonation in Rocket Motors," Los Alamos National Laboratory Rept. LA-8141-MS, Jan. 1980.

18. Charles A. Forest, "A Numerical Model Study of Burning and Detonation in Small PETN-Loaded Assemblies," Los Alamos National Laboratory Rept. LA 8790, Apr. 1981.